Astron. Astrophys. 357, 1035–1044 (2000)

ASTRONOMY AND ASTROPHYSICS

Far infrared spectroscopy of FU Ori objects

ISO-LWS observations⋆

D. Lorenzetti[1,3], T. Giannini[1,2,3], B. Nisini[1], M. Benedettini[3], M. Creech-Eakman[4], G.A. Blake[4], E.F. van Dishoeck[5], M. Cohen[6], R. Liseau[7], S. Molinari[8], S. Pezzuto[3], P. Saraceno[3], H.A. Smith[9], L. Spinoglio[3], and G.J. White[7,10]

[1] Osservatorio Astronomico di Roma, Via Frascati 33, 00040 Monte Porzio, Italy
[2] Istituto Astronomico, Università La Sapienza, Via Lancisi 29, 00161 Roma, Italy
[3] Istituto di Fisica Spazio Interplanetario - CNR Area Ricerca Tor Vergata, Via Fosso del Cavaliere, 00133 Roma, Italy
[4] Division of Geological & Planetary Sciences, California Institute of Technology, Pasadena, CA 91125, USA
[5] Leiden Observatory, P.O. Box 9513, 2300 RA Leiden, The Netherlands
[6] Radio Astronomy Laboratory, 601 Campbell Hall, University of California, Berkeley, CA 94720, USA
[7] Stockholm Observatory, 133 36, Saltsjöbaden, Sweden
[8] IPAC/Caltech, MS 100-22, Pasadena, California, USA
[9] Harvard-Smithsonian Center for Astrophysics, 60 Garden Street, Cambridge, MA 02138, USA
[10] Queen Mary & Westfield College, University of London, Mile End Road, London E1 4NS, UK

Received 12 January 2000 / Accepted 7 March 2000

Abstract. We present the results of the first spectrophotometric observations of a sample of FU Ori objects obtained with the Long Wavelength Spectrometer (LWS) on board the Infrared Space Observatory (ISO). The [OI] (63 μm) and the [CII] (158 μm) lines are commonly observed in all spectra (both ON and OFF source). The observational novelty is the presence in most of the sources of the transition of ionised nitrogen [NII] (122 μm), which is not detected in other objects in a similar evolutionary phase. This line probes low ionisation and low density material not easily traced by other lines. Line intensities and intensity ratios are used along with model predictions to infer the prevailing mechanisms for line excitation. To reconcile our far-infrared spectroscopy with previous knowledge of these objects, the simultaneous presence of two components is required: well localised J-shocks, responsible for the [OI] emission, and an extended low density ionised medium produced by UV photons from the disc boundary layer, responsible for the [NII] and [CII] emission. A few molecular lines (CO, OH, H_2O) associated with relatively cold and dense peaks are revealed and their intensities are in good agreement with the proposed scenario. Other ionic lines ([OIII] and [NIII]) are detected in two sources in the Cyg OB7 region and likely trace the presence of nearby HII regions.

Key words: stars: circumstellar matter – stars: individual: FU Ori – infrared: ISM: lines and bands – infrared: stars

Send offprint requests to: D. Lorenzetti (dloren@coma.mporzio.astro.it)

⋆ ISO is an ESA project with instruments funded by ESA Member States and with the participation of ISAS and NASA

1. Introduction

Understanding the FU Orionis outburst phenomenon is an important step in reaching a coherent picture of the early phases of stellar evolution. Recent review papers (Hartmann et al. 1993; Hartmann & Kenyon 1996; Kenyon 1999; and references therein) point out the increasing observational and theoretical interest in this subject. At present, the widely accepted explanation of the FU Orionis phenomenon is a large increase in the accretion rate through a circumstellar disc surrounding a low luminosity young star (Hartmann & Kenyon 1985). These events make the disc self luminous, with a luminosity which largely exceeds that of the central star. Alternative explanations of the observed features deal with a rotating stellar envelope (Herbig 1989) or a binary origin (Bonnell & Bastien 1992), but the success of the active disc interpretation relies on its ability to provide a consistent explanation for many observational features from optical to radio wavelengths. In particular, a direct view of FU Ori itself by means of IR interferometric observations (Malbet et al. 1998) has allowed to resolve the object and the data are consistent with the standard accretion disc model with an accretion rate of 6 10^{-5} $M_\odot$ yr^{-1}.

Spectroscopic investigations in the optical range reveal strong blue-shifted absorption components (Hα, NaI lines) that imply a mass-loss rate of about 10^{-5} $M_\odot$ yr^{-1} (Croswell et al. 1987). Such powerful winds may cause systematic blueshift of the lines and obscure their double-peaked structure, which is a normal feature of FU Ori systems, well explained by the disc model.

Molecular outflows are a common feature of FU Ori objects (Levreault 1988; Evans et al. 1994) and the derived properties are consistent with mass loss rates of $\sim 10^{-5}$ $M_\odot$ yr^{-1} derived from optical lines.

Table 1. Parameters of the observed FU-Ori.

Source	Spectral Type	L_{bol} ($L_\odot$)	A_v (mag)	Outflow Activity	Distance (pc)	Other Identifications	IRAS Name
RNO1B	F8II	1000	...	CO	850	L1287 - GN 00.33.9	00338+6312
Z CMa	B5-8neq+sh,G3-4	3500	2.8	CO/HH	1150	HD 53179 - MWC165	07013-1128
V346 Nor	F8III	290	...	CO/HH	700	HH57 IRS	16289-4449
(Re13)	...	50	...	HH	700	...	16289-4449
V1057 Cyg	F0-F3II	370	3.0	CO	600	LkHα 190	20571+4403
V1331 Cyg	B05-F0	36	2.4	CO/jet	600	LkHα 120	20595+5009
V1735 Cyg	...	250	10	CO	900	El 1-12	21454+4718

The ionisation level in the environment close to FU Ori objects is low as suggested by the absence of ionised species other than FeII and SII (Hamann 1994; Welty et al. 1992). Also, UV spectroscopy shows the lack of significant veiling of the absorption features, indicating a smaller than expected boundary layer contribution to the UV radiation (Kenyon et al. 1989). Near IR spectroscopy results are also consistent with the disc model because of the smaller line broadening in the IR (Hartmann & Kenyon 1987). Moreover, the IR HI recombination lines (Brα, Brγ, Pfγ) usually observed both in T Tau and in Herbig Ae/Be stars (HAEBE) are not detected in FU Ori's (except two detections of Brγ in Z CMa and V1331 Cyg). The near-IR spectra are dominated by H_2O and CO absorption features (Sato et al. 1992 and references therein).

Although much information on FU Ori-type objects has been derived from optical and near-IR data, far-infrared data are crucial to constrain several aspects. In particular, the presence of an active disc by itself is not sufficient to account for the observed spectral energy distribution (SED) at these wavelengths. Kenyon & Hartmann (1991) proposed a flared disc to explain the excess far-infrared emission, in which part of the radiation emitted from the warmer, inner parts of the disc is reprocessed. However, such models sometimes require strong flarings with very high values of the disc photospheric height with respect to the midplane to fit the data. An alternative explanation is to add an optically thin dust envelope to the model, so that the flaring can be reduced to acceptable levels. This latter model is used to explain the far-infrared emission.

At far-IR wavelengths the IRAS Catalog still represents a major source of information (see also Kenyon & Hartmann 1991 for ADDSCAN fluxes) for both photometry and spectroscopy: the IRAS LRS (IRAS Science Team 1986) reports the (8–22 μm) spectra of three FU Ori objects, namely V883 Ori, Re 50 IRS and Z CMa, where only the silicate absorption band at 9.7 μm is recognizable. Additional far-IR spectra in the range 8–13 μm are available for Z CMa, FU Ori, V1551 Cyg, V1057 Cyg, V1331 Cyg and V1735 Cyg (Cohen & Witteborn 1985; Hanner et al.1998), while the first spectrum at longer wavelengths (2–45 μm) of a FU Ori star (Z CMa) is given in Meeus & Waelkens (1999).

In the sub-mm continuum (350 μm–2mm) the FU Ori class has been surveyed by Weintraub et al. (1991) who found that they are very bright sources often optically thick out to sub-mm (or even mm) wavelengths. Recent results from mapping at 1.3mm at an angular resolution of 10–20 arcsec (Henning et al. 1998) have resolved RNO1B and Z CMa (but not V1331 Cyg) into a core/envelope structure.

The large-scale activity of FU Ori systems is expected to be quite unaffected by the star itself, but is intimately related with interactions between the circumstellar environment and accretion disc events. Since these latter are repetitive on time scales of several thousand years, they are thought to be responsible for intermittent mass loss episodes that produce subsequent (and hence spatially separated) Herbig-Haro manifestations (Reipurth & Raga 1999).

For a significant sample of FU Ori stars we report here for the first time far-IR spectra (45–200 μm) obtained with the long-wavelength spectrometer on board ISO. This spectrometer has the suitable aperture ($\sim$ 80 arcsec) to properly sample the neighbourhood of the FU Ori systems and provides an unbiased spectroscopic survey of these objects in this spectral range. The main aims of the present work are: *i)* to search for FIR ionic and molecular transitions and to understand how their presence (or absence) is related to the properties of the central FU Ori disc; *ii)* to derive from line intensities and intensity ratios the physical properties of the emitting gas; and *iii)* to compare the results with current model predictions in order to constrain the dominant mechanism(s) of the gas excitation.

2. Definition of the sample

Our targets are listed in Table 1 along with some useful parameters: spectral types correspond to the range of values found in the literature, while the other parameters are quite uncontroversial. The selected objects constitute a significant sample, representing $\sim$50% of the dozen known members or candidates. Z CMa has a high luminosity atypical of such stars, but Koresko et al. (1991) showed that the optical component of the Z CMa binary can be a FU Ori object, but that most of the luminosity arises in the infrared companion. The source Re13 is indicated in brackets since it is not a FU Ori object; it is nevertheless included here because its proximity to V346 Nor (distance less than 1 arcmin) forced us to do separate pointings. Both sources are young and belong to the Sa187 dark cloud in Norma; only accurate deconvolution techniques can separate them at far-IR wavelengths (Prusti et al. 1993). The source V1331 Cyg is indeed a FU Ori candidate, or more precisely, an object between outbursts, as defined by McMuldroch, Sargent & Blake (1993).

From Table 1 one can see that all the sources are associated with outflowing material in the form of CO bipolar flows and/or Herbig-Haro jets. ISO-LWS observations of an additional member of this class, L1551-IRS5, and of a related object, SSV13, are reported by White et al. (2000), and by Molinari et al. (2000), respectively.

3. Observations and data reduction

The observations were carried out with the Long Wavelength Spectrometer (LWS: Clegg et al. 1996, Swinyard et al. 1996) on board the Infrared Space Observatory (ISO: Kessler et al. 1996) in full grating scan mode (LWS01 AOT). This configuration provides coverage of the 43–196.7 μm range at a resolution R $\sim$ 200, with an instrumental beam size of $\sim$ 80 arcsec. The spectra were oversampled by a factor of 4 and were processed with the off-line pipeline version 7 (OLP V7). The flux calibration is based on observations of Uranus, resulting in an estimated accuracy of about 30% (Swinyard et al. 1996). The wavelength calibration accuracy is a small fraction ($\approx$25%) of a resolution element, i.e. 0.07 μm in the range 43–90 μm and 0.15 μm in the range 90–196.7 μm. A spectrum is composed of ten subspectra, each from one of the ten detectors. Data reduction steps include: averaging the different spectral scans after removing the glitches due to the impact of cosmic rays and correcting the low-frequency fringes which result from interference along the optical axis with off-axis emission (Swinyard et al. 1996).

An estimate of possible contamination from large scale emission is obtained by taking additional spectra adjacent to the source. In most cases these OFF source measurements were obtained by means of raster maps oriented to sample the outflowing gas. Since the total integration time spent on the OFF positions is comparable to that ON source, the individual map points can be co-added to effectively remove any contribution not related to the central source or they can be separately used to investigate possible local features. Table 2 reports the journal of observations. For each entry, ON or OFF source positions are indicated: in Columns 2 to 7, the coordinates of the pointed position (in the case of a raster map they indicate the map center); the parameters of the raster, namely the number of positions (m$\times$n - Column 8), where m is along the direction of position angle and n perpendicularly; in Column 9 the spacing between the raster position (step) is given; position angle in Column 10; the total integration time (Column 11) obtained by means of a number of subsequent scans (Column 12); finally the date and orbit numbers are given in Columns 13 and 14, respectively.

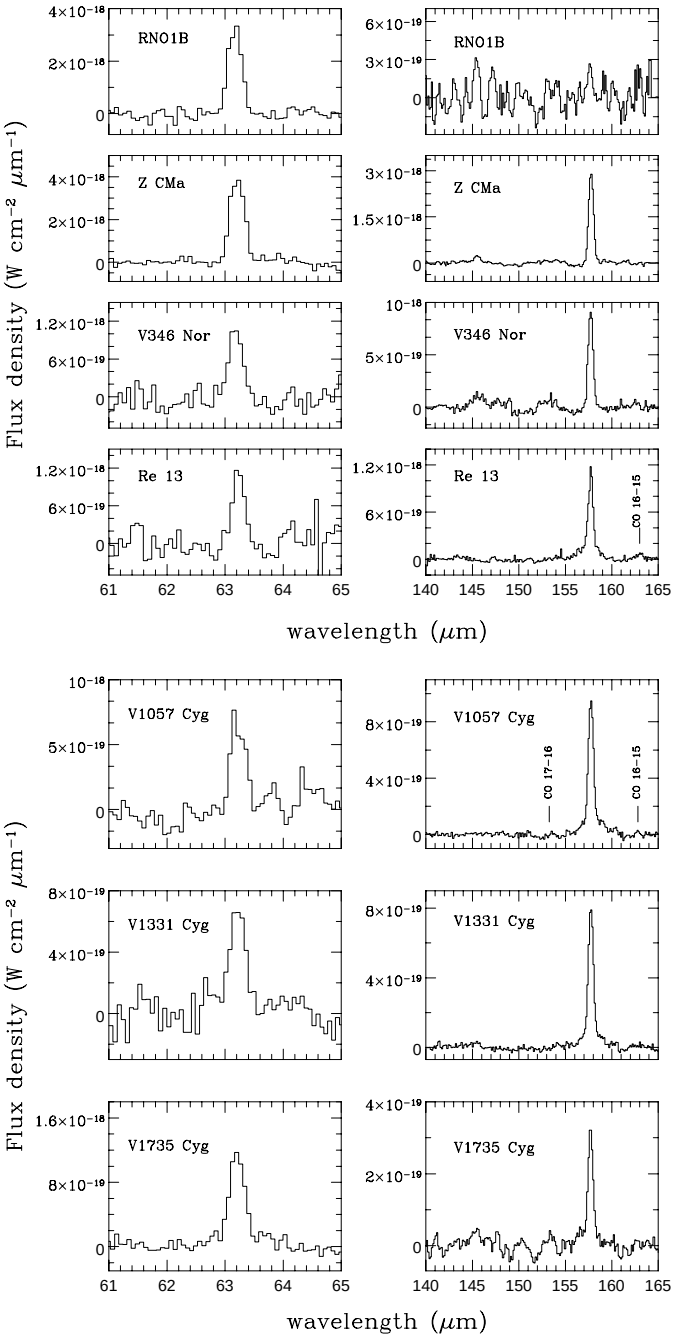

Fig. 1. Continuum subtracted LWS spectra of the observed FU Ori objects, showing selected ranges containing the [OI] (63 and 145 μm) and [CII] (158 μm) lines. Other detected lines are labelled in the appropriate panels.

4. Results

Selected portions of the continuum subtracted LWS spectra are presented for all observed sources in Figs. 1, 2 and 3.

The LWS line analysis is performed on the defringed single detector spectra after subtracting a polynomial function which fitted the continuum using a single gaussian function. The errors on the line intensities correspond to 1σ statistical uncertainties derived from the *rms* fluctuations adjacent to the line. The criteria adopted for line detection are the following: *i)* signal to noise ratio S/N $\geq$ 3; *ii)* distance between observed and rest wavelength comparable to the wavelength calibration accuracy; *iii)* line width compatible with the nominal value of the relative detector ($\approx$ 0.29 and 0.60 μm for the short and long wavelength detectors, respectively). The fluxes of the detected lines ON and OFF source are given in Tables 3 and 4, respectively; these values correspond to the individual pointings indicated in Table 2.

Table 2. Journal of observations

Target	α(1950.0)			δ (1950.0)			raster parameters			t_{int}	n_{scan}	date	orbit
	h	m	s	$^\circ$	$'$	$''$	points	step ($''$)	P.A. ($^\circ$)	(sec)			
RNO1B	00	33	52.1	63	12	24	1	-	-	1088	5	27 Aug 1996	285
RNO1B off	00	33	52.1	63	12	24	2×1	180	53	1654	4	27 Aug 1996	285
Z CMa	07	01	22.5	-11	28	36	1	-	-	2590	14	8 Nov 1997	723
Z CMa NE	07	01	28.4	-11	27	47	1	-	-	1292	6	8 Nov 1997	723
Z CMa SW	07	01	16.6	-11	29	24	1	-	-	1294	6	8 Nov 1997	723
V346 Nor	16	28	56.8	-44	49	08	3×1	50	138	2774	6	31 Aug 1996	289
Re 13	16	28	51.8	-44	49	15	3×1	137	51	2784	6	31 Aug 1996	289
V1057 Cyg	20	57	06.2	44	03	46	1	-	-	2078	12	23 Dec 1997	768
V1331 Cyg	20	59	32.3	50	09	53	1	-	-	2078	12	23 Dec 1997	768
V1735 Cyg	21	45	26.9	47	18	08	1	-	-	4409	24	5 Aug 1996	263
V1735 Cyg off	21	45	26.9	47	18	58	2×1	180	90	4166	12	5 Aug 1996	263

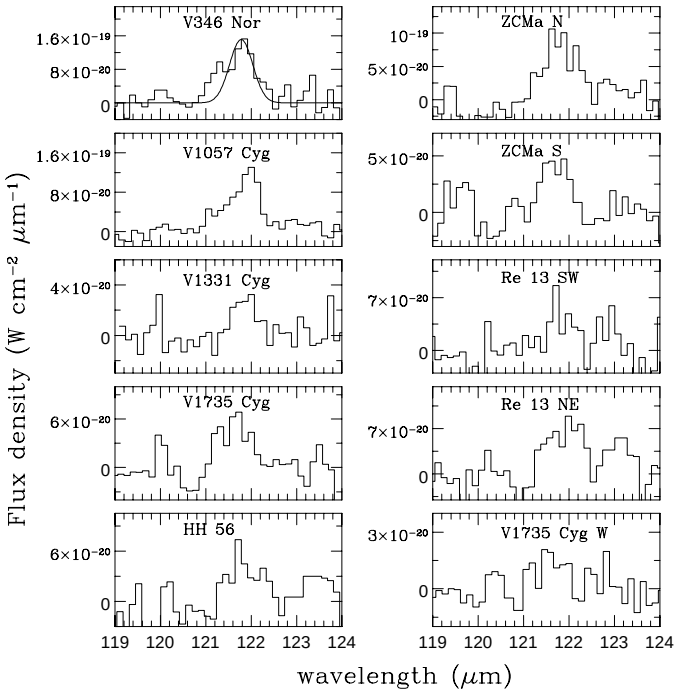

Fig. 2. Continuum subtracted LWS spectra of the observed FU Ori objects, showing selected ranges containing the [NII] (121.8 μm) line at both ON and OFF source positions. The gaussian fit to the line is reported, for convenience, just in the first panel.

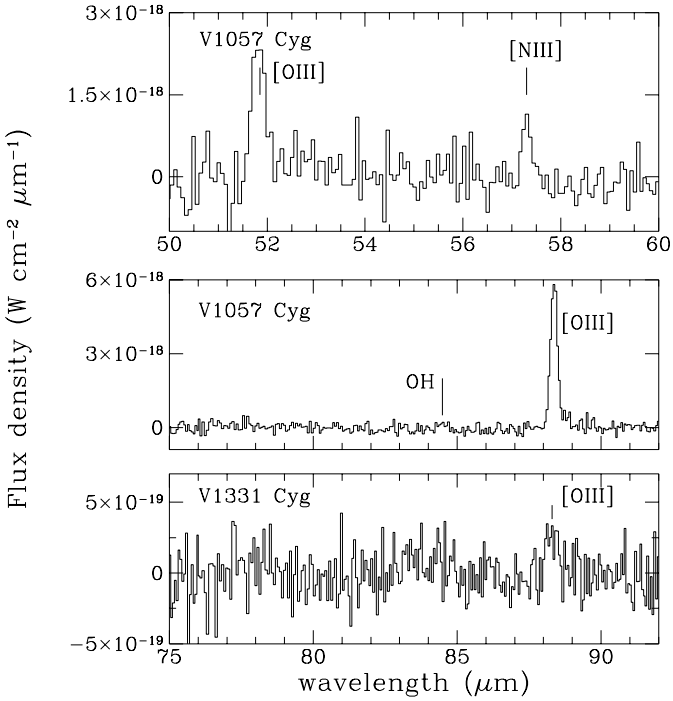

Fig. 3. Continuum subtracted LWS spectra of the observed FU Ori objects V1057Cyg and V1331Cyg containing the [OIII] (51.8 and 88.4 μm) and [NIII] (57.4 μm) lines.

Some upper limits relevant to the following discussion are also reported, and correspond to a 3σ fluctuation of the continuum in the line expected position. From Tables 3 and 4 it can be seen that the [OI] (63, 145 μm) and the [CII] (158 μm) lines are commonly observed in all spectra. The [OI] lines are brighter ON source, while the [CII] line tends to have comparable intensities (within a factor of 2) at all positions. We note that OFF source observations of the same object are often not comparable (within the uncertainties), therefore they cannot be averaged together to obtain a single contribution for a quick ON-OFF evaluation. On the contrary, they often indicate that some emission gradient is present (see Table 4). For instance: *i)* the SW line emission near Z CMa is more intense than that to the NE; *ii)* the higher value of [OI] 63 μm in V346 Nor OFF-NW could be due to the presence of the Herbig-Haro object HH56 in that lobe.

The higher ionisation [NII] line at 121.89 μm is also commonly detected both ON and OFF source (see Tables 3, 4 and Fig. 2). In one case (Z CMa) [NII] line emission is detected only at the OFF positions presumably because the brightness of the source itself prevents to detect weak lines, as confirmed by the upper limit calculated at 122 μm for the ON position (Table 3) which is consistent with the OFF source values (Table 4). By carefully inspecting the [NII] line data (Tables 3,4 and Fig. 2) one can realise that these detections are close to the limits of the observing capabilities, as testified by the large number of

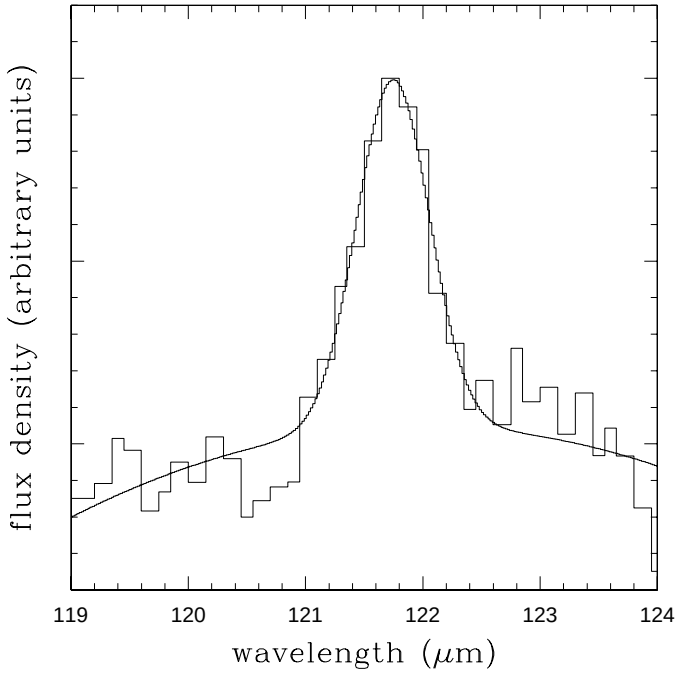

Fig. 4. Mean spectrum in the range 119–124 μm obtained by averaging all the individual spectra depicted in Fig. 2, along with the superimposed formal fit (see text for details).

caution flags reported in the Tables 3 and 4. In particular, a predefined FWHM (equal to the resolution element of 0.60 μm) is used in many cases for the gaussian fitting of the line profile. Such fit, superimposed to the observed spectrum, is depicted, as an example, in the first panel of Fig. 2. The LWS detection of [NII] 122 μm line with LWS is complicated by some concurrent instrumental problems:

i) LWS spectra result from adding up subsequent scans obtained by moving the grating in both forward and reverse direction. Unfortunately the 122 μm wavelength falls within a detector (LW2) where the difference between forward and reverse scans is more evident; this difference originates a displacement of the line center and, consequently, it affects the bandwidth as well.

ii) The problem evidenced before (*i*) could be, in principle, circumvented by considering only the scans in the same direction, but this procedure often prevents to reach the signal to noise value required for a valid detection.

iii) LWS does not offer any redundance for detecting the [NII] line which falls onto a single detector, hence no overlap exists with adjacent detectors, as usually happens for other lines.

iv) The LW2 detector is one among the long wavelength detectors most affected by fringing (Swinyard et al. 1996).

All these facts make arguable the [NII] detections, but the circumstance to find this line pratically at all the pointings on FU Ori objects and their close environment, surely increases the statistical confidence in ascribing this property ([NII] line emission) to this specific class. To emphasize this point, we have constructed a sort of "mean spectrum" in the range 119–124 μm, by averaging all the spectra given in Fig. 2, each normalized to its peak value. The result, reported in Fig. 4, demonstrates that [NII] line is indeed real and that all the other "features" (noise generated) present in the individual spectra, are definitively removed. We have done a formal fit to this [NII] synthetic line (Fig. 4), which provides a detection at S/N=8.3 with a FWHM=0.73 μm and a central wavelength λ_o=121.75 μm. Aware of this novelty, we have *a posteriori* checked a large number of available spectra relative to both PMS objects and OFF source positions search-

Table 3. ON-Source line intensities and few upper limits (see text)

Source	λ_{obs} (μm)	Identification	Flux (10^{-19} W cm^{-2})	Notes
RNO1B	63.16	[OI]	9.6 ± 0.7	
	145.44	[OI]	1.9 ± 0.6	
	157.61	[CII]	1.3 ± 0.4	a
Z CMa	63.20	[OI]	12.4 ± 0.5	
	79.07	OH	1.1 ± 0.4	a,d
	122		< 4.5	
	145.49	[OI]	0.8 ± 0.2	
	157.74	[CII]	18.5 ± 0.2	
V346 Nor	63.16	[OI]	3.9 ± 0.5	
	121.81	[NII]	1.0 ± 0.25	c
	145.49	[OI]	0.6 ± 0.2	c
	157.70	[CII]	6.4 ± 0.2	
Re13	63.27	[OI]	2.8 ± 0.6	a
	157.71	[CII]	7.5 ± 0.3	
	162.68	CO (J=16-15)	0.5 ± 0.15	c
V1057 Cyg	51.83	[OIII]	8 ± 1	
	57.37	[NIII]	3.0 ± 0.3	
	63.21	[OI]	2.0 ± 0.3	
	84.49	OH	1.3 ± 0.5	d
	88.36	[OIII]	18.1 ± 0.06	
	121.91	[NII]	1.0 ± 0.2	c
	145		< 0.3	
	153.37	CO (J=17-16)	0.18 ± 0.07	d
	157.75	[CII]	7.13 ± 0.09	
	162.77	CO (J=16-15)	0.16 ± 0.07	d
V1331 Cyg	52		< 3.0	
	63.21	[OI]	2.3 ± 0.3	
	88.23	[OIII]	1.0 ± 0.3	c
	121.85	[NII]	0.4 ± 0.15	c
	145.47	[OI]	0.19 ± 0.06	
	157.74	[CII]	5.8 ± 0.1	
V1735 Cyg	63.20	[OI]	3.9 ± 0.2	
	121.39	[NII]	0.7 ± 0.25	b,d
	145.49	[OI]	0.22 ± 0.06	c
	157.69	[CII]	2.1 ± 0.1	

Notes:
a – FWHM marginally larger or smaller than the nominal value of the relative detector
b – distance between observed and rest wavelength ($\Delta\lambda$) marginally exceeding the resolution element
c – Line fit obtained with a fixed value of FWHM (0.60 μm)
d – S/N ratio marginally less than 3

ing, with the same criteria, for the presence of the [NII] 122 μm line related both to the central source (ON source pointings), and to galactic emission (OFF source pointings). We note that all these data are currently available since they belong to the ISO archive. We have surveyed about 20 pointings relative to young stellar objects of both low and high mass; 11 HAEBE stars (see the list given in Lorenzetti et al. 1999); 17 Herbig-Haro objects whose "averaged" spectrum, showing no sign of line emission at 122 μm, was presented by Liseau et al. (1997). Our attempts have given always a negative result with the exception of some HII regions (e.g. M8E, NGC6334, S87). In particular, the detection of the [NII] 122 μm line is unusual in HAEBE stars (Lorenzetti et al. 1999), despite of the most favourable spectral types of this latter class. In that paper [NII] emission was found only for the B0 star CoD-42 although other objects have the same ionising capability; the emitting region has been recognized as a dilute optically thin region with low electron density ($n_e < 6\ 10^2$ cm^{-3}), i.e. a region very similar to that proposed (see Sect. 5.2) for explaining the [NII] emission in FU Ori environment, but presumably ionised by stellar photons.

The [NII] 122 μm line is important since it probes low ionisation and low density material not easily studied with other lines, owing to its low ionisation potential (IP = 14.5 eV) and its critical density (n_{cr} = 3 10^2 cm^{-3}). COBE has revealed that [NII] gives the second strongest emission feature from the large scale structure of our Galaxy, after [CII] 158 μm line (Wright et al. 1991; Fixsen et al. 1999). It is noteworthy that the [NII] emission we have observed cannot be considered as galactic background emission because only an upper limit of 0.2 10^{-19} W cm^{-2} in the ISO-LWS beam is expected as contribution from low galactic latitudes (Fixsen et al. 1999), while our observations provide values systematically larger by more than a factor of two; moreover the lack of any [NII] 122 μm detection at other random locations, as discussed above, tends to exclude a significant galactic contribution. In our case, assuming LTE conditions we derive very high NII column densities: a lower limit of $N_{[NII]} \simeq 1.5\ 10^{15}$ cm^{-2} is found assuming that the emitting area fills the LWS beam.

Finally, other ionic lines ([OIII] and [NIII]) are detected in only two sources and likely trace the presence of nearby HII regions, while the few observed molecular transitions (CO, OH, H_2O) are presumably associated with relatively cold and dense peaks of remnant envelopes.

5. Discussion

5.1. [OI], [CII] and [NII] lines

The [OI] 63 μm and [CII] 158 μm fine structure lines are the strongest features observed and can provide, with [OI] 145 μm, a diagnostic of the excitation mechanism. These three lines are essential ingredients of a variety of models that predict the cooling in media characterised by different physical conditions and dominated by different excitation mechanisms. In contrast, none of these models predicts a substantial amount of [NII] emission, whose ubiquitous presence in FU Ori systems represents an observational novelty. In the following, a short analysis of various model predictions will be given, in order to delineate a coherent scenario which can account for the observed properties.

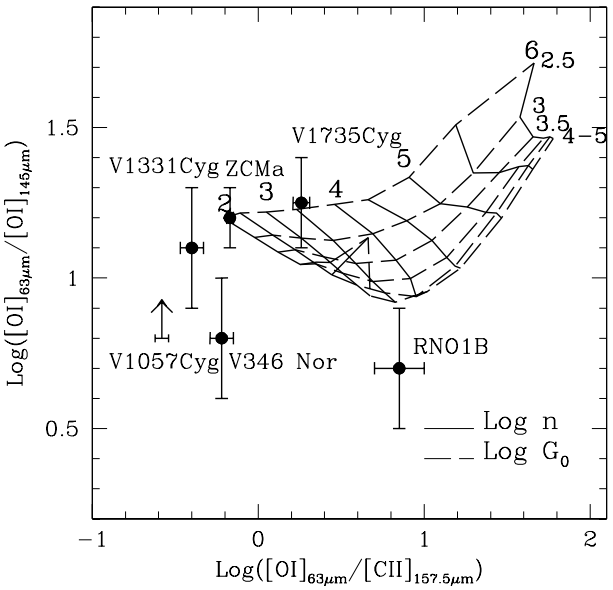

Fig. 5. Observed line ratios superposed on PDR model predictions (Kaufman et al. 1999).

Classical models of photodissociation regions (PDR) (e.g. Tielens & Hollenbach 1985; Hollenbach et al. 1991) are not able to reproduce the observed ratios [OI]63 μm/[CII]158 μm and [OI]63 μm/[OI]145 μm, unless high values of the radiation field $\sim 10^4$ G_o are adopted, where G_o is the average interstellar flux (1.6 10^{-3} erg cm^{-2} s^{-1}, Habing 1968). The comparison with observations is improved by considering the photodissociation model by Kaufman et al. (1999) who include an additional heating source, namely the ejection of photoelectrons from PAHs and very small grains (VSGs). The extra heating source makes a substantial difference since smaller values of both density and radiation field can reproduce a given set of line ratios. Nevertheless, even in such extreme cases, the model predictions are only marginally consistent with the observed line ratios, as depicted in Fig. 5. Further difficulties stem from the fact that the [NII] emission remains unexplained, and observations indicate that PAHs and VSGs are not common ingredients of FU Ori environments (Sato et al. 1990; Brooke et al. 1993).

The role of shocks must also be examined since most of the sources are driving outflowing material. High velocity J-shock models can be divided in two classes, applicable to dense (e.g. Hollenbach & McKee 1989) or to more dilute (Shull & McKee 1979) environments, respectively. While the former predict line ratios of 30–200 for [OI]63/[OI]145, the latter provide values around 10, which are much more compatible with our observations. Both classes predict low amounts of [CII] emission (compared with [OI]63 μm), thus the [OI]63/[CII]158 ratios are always greater than 1 (in several cases by orders of magnitude). This contrasts with our data and should suggest to rule out shock mechanisms, unless the [CII] emission has a completely different origin (see next section). Low density J-shocks (Shull & McKee 1979) are able to explain the presence

Table 4. OFF-Source line intensities

OFF-Source	[OI] 63 μm	[OI] 145 μm	[CII] 158 μm	[NII] 122 μm	Other lines
	Flux (10^{-19} W cm^{-2})				
RNO1B off NE	2.0 ± 0.5 [c]	-	2.5 ± 0.2 [a]	-	CO(J=16-15): 1.2 ± 0.15 [c]
RNO1B off SW	1.3 ± 0.4 [a]	0.4 ± 0.1 [c]	2.1 ± 0.2	-	
Z CMa off NE	3.9 ± 0.6	-	15.1 ± 0.1	0.6 ± 0.2 [c]	
Z CMa off SW	4.2 ± 0.3	0.45 ± 0.10 [c]	18.1 ± 0.3	0.45 ± 0.1	H_2O 179 μm: 1.6 ± 0.3
V346 Nor off SE	2.5 ± 0.4	-	6.6 ± 0.15	-	
V346 Nor off NW (HH56)	3.3 ± 0.6	-	5.8 ± 0.2	0.4 ± 0.1	CO(J=17-16): 0.7 ± 0.1 [b,c]
Re13 off NE (red lobe)	3.0 ± 0.6 [a]	0.78 ± 0.08 [b,c]	6.2 ± 0.2	0.6 ± 0.2	
Re13 off SW (blue lobe)	1.6 ± 0.6	-	5.7 ± 0.1	0.45 ± 0.15	
V1735 Cyg off E	-	-	1.75 ± 0.08 [a]	-	
V1735 Cyg off W	0.5 ± 0.3 [c]	-	1.18 ± 0.05	0.16 ± 0.06[c,d]	

[a] FWHM marginally larger or smaller than the nominal value of the relative detector
[b] distance between observed and rest wavelength ($\Delta\lambda$) marginally exceeding the resolution element
[c] Line fit obtained with a fixed value of FWHM (0.60 μm)
[d] S/N ratio marginally less than 3

Table 5. Mass loss determinations for FU Ori systems

Source	$\dot{M}$([OI]63 μm)	$\dot{M}$(opt/IR)	Ref.
	($M_\odot$ yr^{-1})		
RNO1B	$1.6\ 10^{-5}$	...	
Z CMa	$6.2\ 10^{-5}$	$1.2\ 10^{-4}$ - $2.5\ 10^{-5}$	1
V346 Nor	$7.3\ 10^{-6}$	...	
V1057 Cyg	$2.7\ 10^{-6}$	$\sim 10^{-5}$	2
V1331 Cyg	$4.2\ 10^{-6}$	2–$2.9\ 10^{-6}$	3,4
V1735 Cyg	$1.2\ 10^{-5}$	...	

References: 1. Corcoran & Ray 1997; 2. Croswell et al. 1987; 3. Hamann et al. 1994; 4. Carr 1989.

of NII emission, although with column densities that are much lower than observed. Moreover, in presence of a J-shock, the [OI]63 μm line can be used to derive the mass loss rate from the relationship $\dot{M}_{[OI]63}$ ($M_\odot$ yr^{-1}) = 10^{-6} $L_{[OI]63}/10^{-2}$ $L_\odot$ (Hollenbach 1985). From the data in Table 5 we see that the $\dot{M}$[OI] values are consistent with independent determinations from optical and near IR spectroscopy, thus confirming the plausibility of the J-shock hypothesis. In conclusion, J-shocks seem a valid mechanism to account for the observed [OI] emission by itself.

The C-shocks models (e.g. Draine et al. 1983; Kaufman & Neufeld 1996) do not predict any substantial [CII] emission, but they are able to give a line intensity ratio [OI]63/[OI]145 that is comparable to the observed values under specific gas conditions. The predicted ratio is always greater than 10, but it remains near this value in a narrow range of shock speeds (10–20 km s^{-1} at B_o = 50 μG and 15–30 km s^{-1} at B_o = 100 μG) for a pre-shock density n_H=10^4 cm^{-3}, while, increasing the density, the ratio always exceeds the value of 50. Again these models also do not predict any NII emission.

5.2. A possible interpretation

The discussion above highlights the difficulties that current models have in accounting for the large amount of emission from [CII] and mainly from [NII]. In FU Ori systems, the central star (F-G type) cannot provide the requisite ionising photons (FUV field $G_o \approx 0.1$ at 0.1 pc) for that purpose, but the boundary layer ($T_{eff} \sim 3\ 10^4$ K) radiation is able to generate an Extended, Low Density Warm Ionised Medium (ELDWIM by Petuchowsky & Bennett 1993) where only [NII] (122 and 205 μm) and [CII] are expected to occur. Line emission in ELDWIM is predicted by Petuchowsky & Bennett (1993) and from their data we derive the expected ratio [CII]158/[NII]122 as a function of the electron density N_e. In Fig. 6 this model is reported along with our observed values, which are in good agreement with the prediction and indicate very low values for the electron densities ($N_e \lesssim 100$ cm^{-3}). The intensity ratios found at the OFF source positions Z CMa NE and SW ($\approx$ 30 see Table 4) are not reported in Fig. 6, but they favour nebular rather than solar abundances.

The presence of an ELDWIM in these objects is plausible because the circumstellar matter is mainly concentrated in the disc, while the environment of other PMS objects is characterised by more dense envelope structures. This circumstance can explain why the [NII] emission is so frequently observed only in FU Ori objects. To verify this hypothesis we have evaluated the expected size of the emitting region and the NII column densities, which can both be compared with observational data. Assuming that, for a typical FU Ori object, the stellar mass and radius are M_* = 1 $M_\odot$, R_* = 4 $R_\odot$ (Kenyon et al. 1988) and the accretion rate is $\dot{M}_{acc}$ = 10^{-5}–10^{-4} $M_\odot$ yr^{-1} (Croswell et al. 1987), we derive L_{acc} = $GM_*\dot{M}/2R \simeq$ 40–400 $L_\odot$, which are consistent with the observed values given in Table 1. If we assume that 1/2 of this luminosity is emitted in ionising UV (Thompson 1982), we derive the number of ionising photons per sec. This latter value can be equated to the number of recombinations per sec (in the case of an ionisation bounded nebula) to derive the size of the emitting region. The following assumptions have been adopted: *i*) a density law of the type n(r) = $n_o(R_*/r)^\gamma$, where n_o represents the density at r=4$R_\odot$ and γ the power law exponent, which often is taken less than unity (e.g. Henning et al. 1998). Here we adopt a value n_o = 10^8 cm^{-3} to

be compatible with the low electron densities at large distances derived from our observations, while γ values between 0.9 and 1 are considered. *ii*) The UV field has been extincted by using $A_{UV} \sim 1.5 \cdot A_V$ = 4.5 mag (Cardelli et al. 1989). *iii*) The fractional ionisation = 0.1 (Hamann et al. 1994). As a result we derive an emitting region radius of 0.16 pc, which corresponds (at the typical distance of the FU Ori stars of about 700pc) to $\sim$ 50 arcsec, namely larger than (or comparable to) the ISO-LWS beam radius. In other words the presence of substantial emission in the OFF-source positions is somewhat predictable. For an abundance ratio [N]/[H] $\simeq 7\ 10^{-5}$ (Meyer et al. 1997) and a fractional ionisation $\simeq$ 0.1, we derive an ionised nitrogen column density $N_{[NII]} \simeq 5\ 10^{15}$ cm^{-2}, quite comparable to that estimated by our observations (Sect. 4).

Such a scenario apparently contradicts the lack of optical NII, or other ionised lines, but at the very low temperatures typical of these HII regions (T $\sim$ 4000 K - Heiles 1994) only far-IR fine structure lines are expected to be excited. Finally, we remark that in the FU Ori envelopes there is certainly present also neutral material, as revealed by low-J CO transitions.

From our oversimplified ionisation model we can estimate that the neutral mass contained in the ELDWIM is $\simeq$ 0.7 $M_\odot$. This value can be compared with other determinations available in the literature, although some caution is required because of the large differences in the employed apertures which sample different environments. It is noteworthy that FU Ori objects are presumably located at the external edge of dense cloud cores, as indicated by the low values of the extinction toward them; hence (sub)mm observations tend to include larger background contributions than our model, which, of course, ignores such morphology. Nonetheless, we can see that our estimate of 0.7 $M_\odot$ within a radius of 0.16 pc is consistent with the solar mass or more of molecular and neutral material found in the envelope of V1331 Cyg (McMuldroch et al. 1993) and V1057 Cyg (McMuldroch 1999). An opposite, but illustrative case is represented by RNO1C (nearby component of RNO1B, unresolved by LWS). Yang et al. (1991) give values of 130 $M_\odot$ and >10 $M_\odot$ for the surrounding cloud within radii of 0.6 and 0.12 pc, respectively; these results suggest a very sharp central mass concentration which should prevent the ionising photons to escape and, in turn, the ELDWIM to be formed. Our observations support this view since RNO1B is the unique source in our sample that shows no evidence of [NII] emission, at both ON and OFF source positions.

The lack of [NII] detection in HAEBE stars could be due to the different nature of their envelopes which are much denser than the [NII] 122 μm critical density and present a higher ionisation level, making this line practically undetectable.

In conclusion we propose two simultaneously active mechanisms for far-IR line excitation: localised shocked regions associated with outflowing gas (CO and/or HH objects) responsible for the [OI] emission and an extended low density ionised medium where [CII] and [NII] originate. A PDR contribution to [OI] and [CII] emission may be present, but does not seem to dominate.

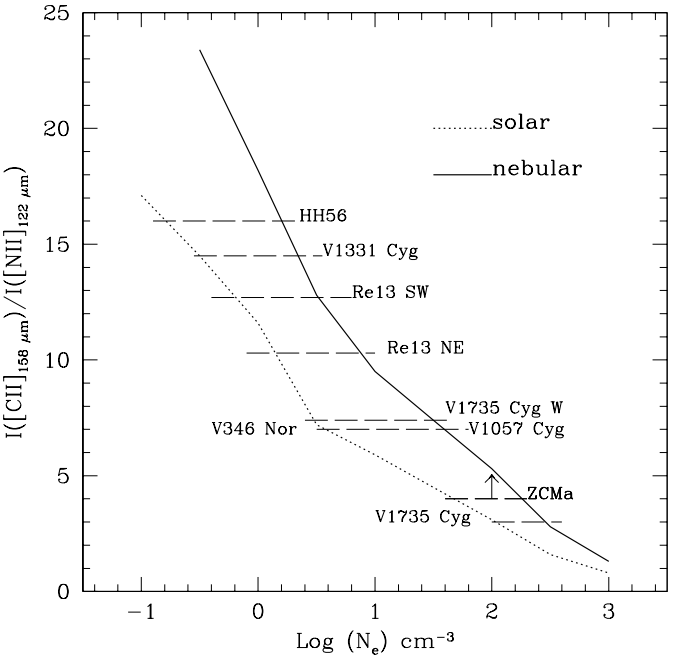

Fig. 6. Observed [CII]/[NII] ratios superimposed on Petuchowsky & Bennett (1993) models by considering solar or nebular abundances.

5.3. Other ionised lines

Lines from highly ionised species are associated with the sources V1057 and V1331 Cyg. Both belong to the Cyg OB7 association as depicted in the large scale view of the molecular clouds in Cygnus given by Dobashi et al. (1994), whose maps are very effective in illustrating the distribution of the OB supergiants and how they relate to the different young sources present in that region.

5.3.1. The case of V1057 Cyg

The source V1057 Cyg lies in a dense dust pocket in the HII region NGC 7000 (Herbig 1977), thus the observed lines from ionised species NII, NIII, OIII are likely related with the local environment more than with the source itself. Note that no OFF source observations were obtained for this object. According to Rubin et al. (1994) (R94), far-IR lines are good tracers of both the electron density and density gradients, hence from the observed ratio [OIII] 88/52 we can derive a very low value of the electron density N_e[OIII] $\lesssim$10 cm^{-3} (independent of the temperature). Assuming N_e[OIII] $\simeq$ N_e[NIII], and taking N_e[NII] $\simeq$ 30 cm^{-3} from Fig. 5, we can estimate the fractional ionisation:

$$\frac{\langle N^{++}\rangle}{\langle N^{+}\rangle} = \frac{F_{57}/\epsilon_{57}}{F_{122}/\epsilon_{122}} = 0.6 \pm 0.2 \qquad (1)$$

where ϵ_λ = $j_\lambda/(N_e N_i)$, j_λ is the volume emissivity for the line and N_i is the ion density. The ϵ values are given in R94 as a function of N_e. In the ionisation bounded case, a value of 0.6 for the nitrogen fractional ionisation would imply T_{eff} $\simeq$ 36500–37000 K, in agreement with the spectral type O6

of the exciting star HD199579 (Humphrey 1978) at the projected distance of 8.1 pc. With the given parameters, the photoionisation code CLOUDY (Ferland 1996) confirms our findings, providing values very close to unity for the ratios R = Log(Lum$_{obs}$)/Log(Lum$_{cloudy}$) (R$_{[OIII]52}$ = 1.000; R$_{[OIII]88}$ = 1.003; R$_{[NIII]57}$ = 0.993). Moreover, we have used [NIII] and [OIII] lines to infer the N/O abundance in the HII region. It is well known that estimates derived from far-IR lines are usually higher than those obtained from optical lines, but the far-IR method has been found more adequate in providing reliable N/O ratios (Rubin et al. 1988). Following their method and taking the j_{57}/j_{52} ratio from Lester et al. (1987), we have:

$$N/O = \frac{N^{++}}{O^{++}} = \frac{F_{57}/j_{57}}{F_{52}/j_{52}} = 0.65 \pm 0.15 \quad (2)$$

Our determination is in good agreement with 0.56 $\pm$ 0.1 (R94) which is the mean value derived from a sample of 13 galactic HII regions (4 times greater than the mean optical value - Rubin et al. 1998).

We should note that, in principle, fast shocks (at velocities $\gtrsim$100 km s^{-1}) are able to produce [NII], [NIII] and [OIII] emission (Raymond 1979). However this prediction deals with only optical lines and provides for the ratios between NIII and NII column densities values which are much lower than that suggested by our observations [see Eq. (1)].

5.3.2. The case of V1331 Cyg

This source is also close (projected distance $\approx$ 15 pc) to an ionising B1 star (HD 199216) to which the [OIII] 88 μm line is likely attributable. Indeed CLOUDY predicts R$_{[OIII]88}$ = 1.001. Unfortunately, the upper limit on the [OIII] 52 μm line (see Table 3) does not give (R94) a strong constraint on the electron density, namely N$_e < 10^3$ cm^{-3}, a value which is not in contrast with the value from Fig. 6.

5.4. Molecular emission

We have detected only few molecular lines at five positions, namely toward RNO1B NE, Z CMa ON and SW, V346 Nor NE and V1057 Cyg (see Tables 3 and 4). Although molecular emission at far-IR wavelengths does not seem a relevant characteristic of this class, it gives nevertheless additional and compelling information about the prevailing excitation mechanism.

Let us first examine the case of V1057, where three lines are observed (CO and OH). The CO J=17-16 and J=16-15 very likely trace the peak of the CO line intensity distribution (as a function of the rotational quantum number). In that case we can derive (McKee et al. 1982) plausible ranges for the physical conditions: for any value of the temperature T $\geq$ 250 K, the density is always higher than 10^6 cm^{-3}. This indicates that the molecular emission comes from high density peaks or knots, and likely represents the cooling of shock excitation. J-shocks (Hollenbach & McKee 1989) appear to be preferred with respect to C-shocks (Draine et al. 1983; Kaufman & Neufeld 1996), since the former models predict that for shock velocities v$_s$ $\simeq$ 30–40 km s^{-1}, and pre-shock densities n $\sim 10^5$ cm^{-3}, the OH (84 μm) emission is larger than the CO J=17-16 and J=16-15 lines, as observed, and that OH emission dominates over H_2O, which remains indeed undetected. Moreover we note that pre-shock densities of $\sim 10^5$ cm^{-3} are compatible with values derived from observations, by assuming a compression factor ($n_{post-shock}/n_{pre-shock}$) of 10. C-shock models predict similar ranges for v$_s$ and n, but are not able to give OH (84 μm) > CO J=17-16, J=16-15. This comparative picture between J and C shocks properties is complicated in our cases because of the presence of an UV field. If this field is present, the H_2O could be photodissociated to OH, making a real C-shock looking like a J one. Hence the molecular emission seems to support J rather than C type shocks, as already indicated in the discussion concerning fine structure lines (Sect. 5.1), but the presence of the UV field does not allow C shocks to be excluded.

The same CO lines have also been detected in the RNO1B NE and V346 Nor NE positions. Both of them exactly coincide with the lobes of CO outflows, in particular the latter position includes the Herbig-Haro object HH56. Therefore, conditions similar to those described above are likely traced.

Finally, the revealed molecular emission in Z CMa agrees well with the proposed interpretation. While OH (79 μm) is observed ON source, H_2O (179 μm) is observed at the SW positions, namely along the jet emanating from the central source (Poetzel et al. 1989). Both lines are close to the fundamental transitions and, as such, indicate a low level of excitation. Therefore it appears quite natural to find OH, a product of water vapour photodissociation, closer than H_2O to a very luminous central object.

5.5. Far-IR continuum variation?

Because of their activity related to disc accretion phenomena, the FU Ori objects represent one of the most suitable class for which it is worthwhile to search for evidence of variability at far-IR wavelengths. ISO-LWS spectrophotometry is ideally suited to have a check more than ten years after the IRAS flight. We have simulated IRAS-like filters to derive the LWS fluxes densities at the same effective wavelengths of 60 and 100 μm. Within the uncertainties, no meaningful variation has been detected with the marginal exception of RNO1B, whose 60 and 100 μm fluxes are increased by about 30 and 70% respectively. Moreover we can give for V1057 Cyg a reliable value of 75 $\pm$ 22 Jy for its 100 μm flux, which was not provided by IRAS. LWS data offer the further advantage to establish that the line emission represents only a marginal contribution (always less than 1%) to the broad-band continuum flux.

6. Conclusions

The main conclusions from this work can be summarised as follows:

– ISO-LWS observations have allowed us to obtain the first detection of far-IR fine structure and molecular lines for a significant sample of FU Ori systems.

- The [OI] 63 μm and [CII] 158 μm lines are observed in all sources. While the [OI] emission is more intense ON source, the [CII] tends to have comparable intensities at nearby OFF positions as well.
- The [NII] 122 μm line is commonly observed in FU Ori objects and this circumstance represents a real novelty among all the PMS objects studied by ISO-LWS.
- Predictions from current models are examined to reconcile our results with the present knowledge of these objects. It appears very likely that shock excitation in knots along outflowing matter is responsible for the [OI] emission, while [CII] and [NII] originate in a more extended and dilute medium where a low degree of ionisation is due to UV photons arising from the disc-star boundary layer.
- The few molecular transitions (CO, H_2O, OH) detected confirm our proposed view, and presumably represent the cooling of J-shock excitation, although a C-shock could be masked by the presence of the UV field.
- Two sources, belonging to the same OB association, exhibit [OIII] and [NIII] emission which appears related with the environment rather than with the FU Ori source itself.
- An analysis of the ISO continua at 60 and 100 μm indicates that no significant variation exists with respect to the IRAS values, and, more importantly, that line contributions never affect the broad-band flux density determinations.

References

Bonnell I., Bastien P., 1992, ApJ 401, L31
Brooke T.Y., Tokunaga A.T., Strom S.E., 1993, AJ 106, 656
Cardelli J.A., Clayton G.C., Mathis J.S., 1989, ApJ 345, 245
Carr J.S., 1989, ApJ 345, 522
Clegg P.E., Ade P.A.R., Armand C., et al., 1996, A&A 315, L38
Cohen M., Witteborn F.C., 1985, ApJ 294, 345
Corcoran P., Ray T.P., 1997, A&A 321, 189
Croswell K., Hartmann L., Avrett E.H., 1987, ApJ 312, 227
Dobashi K., Bernard J.P., Yonekura Y., Fukui Y., 1994, ApJS 95, 419
Draine B.T., Roberge W.G., Dalgarno A., 1983, ApJ 264, 485
EvansII N.J., Balkum S., Levreault R.M., Hartmann L., Kenyon S., 1994, ApJ 424, 793
Ferland G.J., 1996, Hazy, a Brief Introduction to Cloudy. University of Kentucky, Dept. of Physics and Astronomy, Internal Report
Fixsen D.J., Bennett C.L., Mather J.C., 1999, ApJ 526, 207
Habing H.J., 1968, Bull. Astr. Inst. Netherlands 19, 421
Hamann F., 1994, ApJS 93, 48
Hamann F., Simon M., Carr J.S., Prato L., 1994, ApJ 436, 292
Hanner M.S., Brooke T.Y., Tokunaga A.T., 1998, ApJ 502, 871
Hartmann L.W., Kenyon S.J., 1985, ApJ 299, 462
Hartmann L.W., Kenyon S.J., 1987, ApJ 322, 293
Hartmann L.W., Kenyon S.J., 1996, ARA&A 34, 207
Hartmann L.W., Kenyon S.J., Hartigan P., 1993, In: Levy E.H., Lunine J.I. (eds.) Protostars and Planets III, Univ. Arizona Press, p. 497
Heiles C., 1994, ApJ 436, 720
Henning Th., Burkert A., Launhardt R., Leinert Ch., Stecklum B., 1998, A&A 336, 565
Herbig G.H., 1977, ApJ 217, 693
Herbig G., 1989, In: Reipurth B. (ed.) Proc. of ESO Workshop on Low Mass Star Formation and Pre-Main Sequence Objects, p. 233
Hollenbach D., 1985, Icarus 61, 36
Hollenbach D., McKee C.F., 1989, ApJ 342, 306
Hollenbach D., Takahashi T., Tielens A.G.G.M., 1991, ApJ 377, 192
Humphrey R.M., 1978, ApJS 38, 309
IRAS Science Team, 1986, A&AS 65, 607
Kaufman M.J., Neufeld D.A., 1996, ApJ 456, 611
Kaufman M.J., Wolfire M.G., Hollenbach D., Luhman M.L., 1999, ApJ 527, 795
Kenyon S.J., 1999, Lada C.J., Kylafis N.D. (eds.) The origin of stars and planetary systems. NATO-ASI Kluwer, p. 613
Kenyon S.J., Hartmann L.W., 1991, ApJ 383, 664
Kenyon S.J., Hartmann L.W., Hewett R., 1988, ApJ 325, 231
Kenyon S.J., Hartmann L.W., Imhoff C.L., Cassatella A., 1989, ApJ 344, 925
Kessler M., Steinz J.A., Anderegg M.E. et al., 1996, A&A 315, L27
Koresko C.D., Beckwith S.V.W., Ghez A., Matthews K., Neugebauer G., 1991, AJ 102, 2073
Lester D.F., Dinerstein H.L., Werner M.W. et al., 1987, ApJ 320, 571
Levreault R.M., 1988, ApJ 330, 897
Liseau R., Giannini T., Nisini B., et al., 1997, In: Reipurth B., Bertout C. (eds.) Herbig-Haro Flows and the Birth of Low Mass Stars. IAU Symp.182, Kluwer Academic. Publ., p. 111
Lorenzetti D., Tommasi E., Giannini T., et al., 1999, A&A 346, 604
Malbet F., Berger J.-P., Colavita M.M., et al., 1998, ApJ 507, L149
McKee C.F., Storey J.W., Watson D.M., Green S., 1982, ApJ 259, 647
McMuldroch S., 1999, Ph.D. Thesis
McMuldroch S., Sargent A.I., Blake G.A., 1993, AJ 106, 2477
Meeus G., Waelkens C., 1999, In: Cox P., Kessler M.F. (eds.) The Universe as seen by ISO. ESA SP-427, p. 373
Meyer D.M., Cardelli T.A., Sofia U.J., 1997, ApJ 490, L103
Molinari S., Noriega-Crespo A., Ceccarelli C., et al., 2000, ApJ in press
Petuchowsky S.J., Bennett C.L., 1993, ApJ 405, 591
Poetzel R., Mundt R., Ray T.P., 1989, A&A 224, 13
Prusti T., Bontekoe Tj.R., Chiar J.E., Kester D.J.M., Whittet D.C.B., 1993, A&A 279, 163
Raymond J.C., 1979, ApJS 39, 1
Reipurth B., Raga A.C., 1999, In: Lada C.J., Kylafis N.D. (eds.) The origin of stars and planetary systems. NATO-ASI Kluwer, p. 267
Rubin R.H., Martin P.G., Dufour R.J., et al., 1998, ApJ 495, 891
Rubin R.H., Simpson J.P., Erickson E.F., Haas M.R., 1988, ApJ 327, 377
Rubin R.H., Simpson J.P., Lord S.D. et al., 1994, ApJ 420, 772 (R94)
Sato S., Nagata T., Tanaka M., Yamamoto T., 1990, ApJ 359, 192
Sato S., Okita K., Yamashita T., et al., 1992, ApJ 398, 273
Shull J.M., McKee C.F., 1979, ApJ 227, 131
Swinyard B.M., Clegg P.E., Ade P.A.R., et al., 1996, A&A 315, L43
Thompson R.I., 1982, ApJ 257, 171
Tielens A.G.G.M., Hollenbach D., 1985, ApJ 291, 722
Weintraub D.A., Sandell G., Duncan W.D., 1991, ApJ 382, 270
Welty A.D., Strom S.E., Edwards S., Kenyon S.J., Hartmann L.W., 1992, ApJ 397, 260
White G.J., Liseau R., Men'shchikov A., et al., 2000, A&A submitted
Wright E.L., Mather J.C., Bennett C.L., et al., 1991, ApJ 381, 200
Yang J., Umemoto T., Iwata T., Fukui Y., 1991, ApJ 373, 137